Hindawi Publishing Corporation
Journal of Nanomaterials
Volume 2013, Article ID 851417, 8 pages
http://dx.doi.org/10.1155/2013/851417

Research Article

Fabrication of TiO_2@Yeast-Carbon Hybrid Composites with the Raspberry-Like Structure and Their Synergistic Adsorption-Photocatalysis Performance

Dang Yu, Bai Bo, and He Yunhua

Environmental Science & Engineering College, Chang'an University, Xi'an 710054, China

Correspondence should be addressed to Bai Bo; baibochina@163.com

Received 17 July 2013; Revised 27 August 2013; Accepted 28 August 2013

Academic Editor: Mengnan Qu

In the present work, we report the preparation and photocatalytic properties of TiO_2@yeast-carbon with raspberry-like structure using a pyrolysis method. The products are characterized by field emission scanning electron microscopy (FE-SEM), energy dispersive spectrometry (EDS), X-ray diffraction (XRD), thermal gravimetric and differential thermal analysis (TGA-DTA), Fourier transformed infrared spectroscopy (FT-IR), and ultraviolet visible spectroscopy (UV-VIS), respectively. The results show that the hybrid TiO_2@yeast-carbon microspheres have ordered elliptic shapes of uniform size (length = 3.5 ± 0.3 μm; width = 2.5 ± 0.5 μm). UV-VIS ascertains that the as-prepared microspheres possess an obvious light response in a wide range of 250–400 nm. In the decomposition of typical model pollutants including methylene blue and congo red, the hybrid composites exhibited excellent photocatalytic activity for the methylene blue due to the enhanced adsorption ability. Further investigation reveals that the combined effect of adsorption from the yeast-carbon core and photocatalytic degradation from the attached TiO_2 nanoparticles were responsible for the improvement of the photocatalytic activities. Hereby, the raspberry-like TiO_2@yeast-carbon has promising applications in water purification.

1. Introduction

In the past few years, raspberry-like composite particles with well-defined structures have become the subject of rapidly growing interest due to their high surface roughness and potential applications [1, 2]. The unique raspberry-like composites have combined excellent characteristics of host particles and guest particles, such as higher surface area, increased chemical and biological stability, rich surface chemical component, and different magnetic or optical properties [3].

The high surface area, large pores (macroporosity), and the presence of surface hydroxyl groups make carbon substance an ideal catalyst support [4–6]. Like the titania photocatalysts supported on the carbon matrix by means of several strategies [7–9] appear to have various benefits and advantages for providing a cheap and effective wastewater treatment and remediation options [10, 11]. For example, Hu et al. [12] obtained TiO_2 nanoparticles/carbon nanotubes particles with raspberry-like structure by combining sol-gel and electrospinning methods. Liu et al. [13] demonstrated the formation of TiO_2/carbon fibers (ACFs) composite photocatalyst via sol-gel method and the TiO_2/ACFs is especially helpful for the removal of low molecular weight organic pollutants in the contaminated water. Areerachakul et al. [14] prepared well-structured TiO_2/granular-activated carbon (GAC) hybrid particles. The TiO_2/GAC showed excellent capabilities in decomposing the herbicide of metsulfuron-methyl (MM) from waste water. In brief, using carbon materials above-mentioned as catalyst supports has increased the photodegradation rate by progressively allowing an increased quantity of substrate to come in contact with the TiO_2 by means of adsorption. In this respect, carbon matrix has been proven to be an invaluable support in promoting the photocatalytic process [15–17] through providing a synergistic effect by creating a common interface between both the carbon phase and the TiO_2 nanoparticle phase. Such synergistic effect can be explained as an enhanced adsorption

of the target pollutant onto the carbon phase followed closely by a transfer through an interphase to the TiO_2 phase, giving a complete photodegradation process [18].

The yeast-carbon is a porous and amorphous solid carbon material, which is derived mainly from baker's yeast. For instance, Nacoo and Aquarone [19] reported the fabrication of yeast-carbon by carbonizing in a gas-heated muffle. The obtained yeast-carbon possessed higher surface area. Similarly, Guan et al. [20] synthesized amphiphilic porous hollow carbonaceous materials via mild hydrothermal treatment of yeast cells. The resultant carbon material displayed effective adsorption of organic chemicals in wastewater treatment. Thus, in the present study, a novel TiO_2@yeast-carbon microsphere with raspberry-like morphology was fabricated firstly by a single-step strategy based on the pyrolysis method. The obtained hybrid microspheres were characterized by FE-SEM, EDS, XRD, TGA-DTA, FT-IR, and UV-VIS, respectively. A possible mechanism for the formation of the composite microspheres was proposed. In addition, the synergistic effect of adsorption-photocatalysis performance in the TiO_2@yeast-carbon microspheres was evaluated by examining the decolonization of methylene blue and congo red.

2. Materials and Methods

2.1. Materials. The powdered yeast was purchased from Angel Yeast Company. Photocatalyst was TiO_2 from Degussa and was used without further purification. In all preparations, absolute ethanol and double-distilled water were used. Methylene blue (MB) and congo red (CR) were analytic grades and were used as the model pollutants in present work.

2.2. Preparation of Raspberry-Like TiO_2@Yeast-Carbon Hybrid Microspheres. In a typical synthesis procedure, 125.0 mg yeast powder was washed with distilled water and absolute ethanol for three times, respectively. The yeast was dissolved in 20.0 mL of distilled water and stirred vigorously for 30 minutes. The pH was adjusted to approximately 3 by adding drop wise sulfuric acid. Further, 10.0 mg TiO_2 was dispersed in 20.0 mL of distilled water, using ultrasonic vibration for 1.0 minute. The pH was adjusted to approximately 9-10 with sodium hydroxide and stirred for 30.0 min. Then the suspended TiO_2 and yeast were gathered by centrifugation from their own suspensions and redistributed in 20.0 mL of distilled water. Afterwards, TiO_2 and yeast suspensions were mixed and magnetically stirred for 1.5 h at room temperature and left for 3.0 h without further stirring or shaking to ensure the formation of TiO_2@yeast particles. Thus, the mixture was centrifuged in three or more cycles to remove the undesired components and finally desiccated at 353 K for 1.0 h. Subsequently the TiO_2@yeast particles were calcined at 573 K for 1.0 h in a nitrogen pipe furnace and cooled to room temperature. After that, the TiO_2@yeast-carbon composite microspheres were obtained.

2.3. Sample Analysis. Philips XL-30 field emission scanning electron microscope (FE-SEM) was used to observe the morphology of samples. X-ray diffraction (XRD) patterns were collected on X. Pert Pro diffractometer using Cu Kα radiation (λ = 0.15418 nm) at a scanning rate of 10°/min. Thermal gravimetric analysis and differential thermal analysis (TGA-DTA) were carried out on an EXSTAR apparatus at a heating rate of 40°/min in flowing high purity N_2. Fourier-transform infrared spectroscopy measurements (FT-IR) were recorded with a Bio-Rad FTS135 spectrometer in the rage of 370–4000 cm^{-1}. UV-VIS diffuse reflectance spectra (UV-VIS) were measured on a HITACHI 340 UV-VIS spectrophotometer.

2.4. Photocatalytic Activity. The methylene blue (MB) dye and congo red (CR) are widely used in dye industry. Therefore, the elimination of these compounds is becoming an increasingly important environmental problem. Photocatalytic degradation of MB and CR was evaluated under UV irradiation in an aqueous media. The initial concentration of MB and CR was set as 2~3 mg/L, respectively. The amount of photocatalysts including yeast-carbon and TiO_2@yeast-carbon were kept at 0.25 g/L. Before UV irradiation, the suspension containing photocatalyst, MB, and CR was deposited within 50.0 min to establish adsorption-desorption equilibrium. Then the suspension was irradiated under a UV lamp (the intensity of irradiation is 60 W). The concentration of MB and CR was traced by UV-VIS spectroscopy. The absorbance characteristic at bands 666.4 nm and 499.0 nm was taken to determine MB and CR concentration by using a calibration curve, respectively.

3. Results and Discussion

3.1. Materials Characterization. The shape and structure of the samples are shown in Figure 1. The SEM image in Figure 1(a) shows that the prime yeast cells have a regular ellipsoidal shape with a diameter varying between 2.6 and 3.7 μm. Figure 1(b) shows an image of the precursor of TiO_2@yeast-carbon. Compared with the bared yeast, the size of the TiO_2@yeast (length = 3.7 ± 0.4 μm; width = 2.6 ± 0.5 μm) was gently increased due to the attachment of TiO_2 nanoparticles. The picture in Figure 1(d) shows an overall image of the TiO_2@yeast-carbon microspheres. The particles maintained the shape of the original precursor and had the average diameter (length = 3.7 ± 0.3 μm; width = 2.5 ± 0.5 μm). Further, higher resolution image in Figure 1(f) shows that the nano-sized TiO_2 particles randomly decorated the surface of yeast spheres, which have the morphology of raspberry-like composites. Similar morphology has been reported for the synthesis of the raspberry-like PMMA/SiO_2 hybrid microspheres [21]. Moreover, the nanoparticles TiO_2 were relatively dispersed on the yeast-carbon in comparison with the agglomerated TiO_2 in the TiO_2/spherical activated carbons composed by Oh et al. [22]. In addition, the raspberry-like morphology of the TiO_2@yeast-carbon microspheres can be confirmed through the EDS analysis. In the insert image in Figure 1(f), the sample contained Ti, C, O,

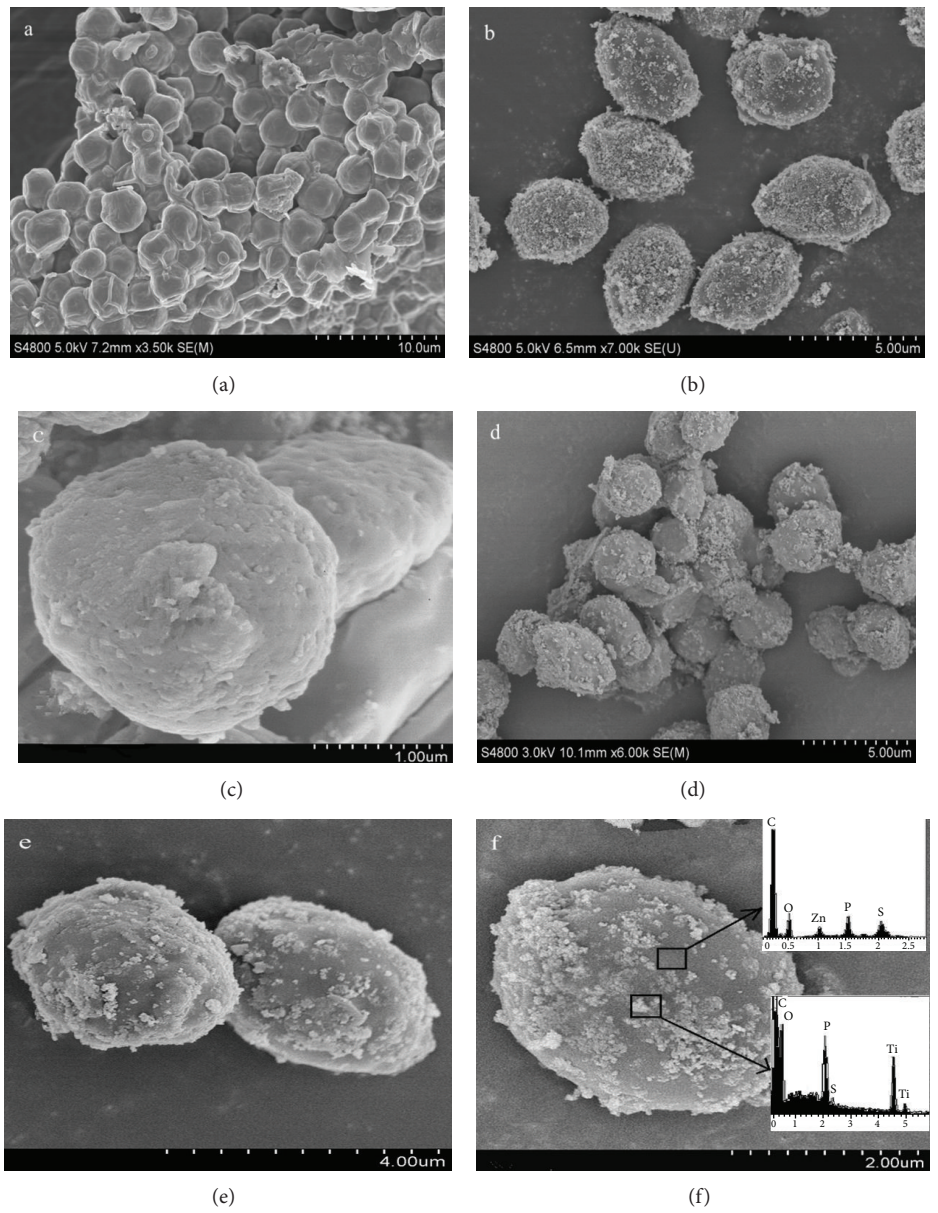

Figure 1: SEM images of (a) the naked yeast, (b) general observation of the raspberry-like TiO_2@yeast precursor, (c) the yeast-carbon, (d) the overall view of the raspberry-like TiO_2@yeast-carbon microspheres, (e) the selected raspberry-like TiO_2@yeast-carbon microspheres, and (f) typical raspberry-like TiO_2@yeast-carbon microspheres observed under high magnification.

S, and P; no other impurity element is detected, confirming that the TiO_2 particles were coated on the surface of the yeast-carbon. By comparing the TiO_2@yeast precursor with the TiO_2@yeast-carbon product, it can be seen that the color of particles changed from pure white to ash black. Thus, it can be inferred that the carbonization of the yeast occurred in the pyrolysis process. In this respect, the control experiments of the yeast-carbon without the attachment of nanoparticles TiO_2 have been conducted under the same conditions. The image of yeast-carbon in Figure 1(c) indicates that the yeast-carbon with an average diameter (length $= 3.5 \pm 0.4\,\mu$m; width $= 2.3 \pm 0.50\,\mu$m) has smooth surface morphology and rich pore structure, which contrasts with the morphology of yeast-carbon synthesized by Shen et al. [23] in which a relatively high distribution of broken shells was observed.

XRD patterns of yeast, yeast-carbon, TiO_2@yeast-carbon, and TiO_2 are displayed in Figure 2. The broad peak around $2\theta = 20^\circ$ indicates that the yeast carbon (in Figure 2(a)) and the yeast (in Figure 2(b)) can be assigned to amorphous species. In Figures 2(c) and 2(d) display the XRD patterns of the hybrid TiO_2@yeast-carbon. The broad peaks centering at $2\theta = 25^\circ$, 37°, 48°, 55°, and 63° are assigned to anatase-type TiO_2 (JCPDS. No: 21-1272) [24]. Other diffraction peaks are in good agreement with diffraction peaks of rutile-type

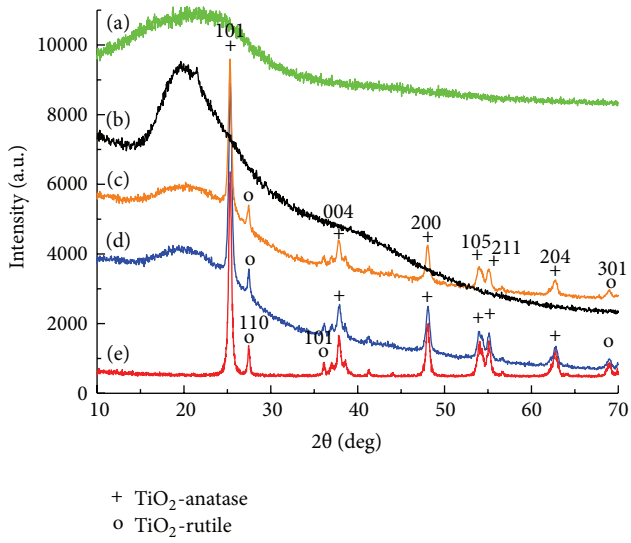

Figure 2: XRD patterns of (a) the prepared yeast-carbon, (b) the premier yeast, (c) the 80% of TiO_2@yeast-carbon, (d) the 40% of TiO_2@yeast-carbon, and (e) the pure TiO_2.

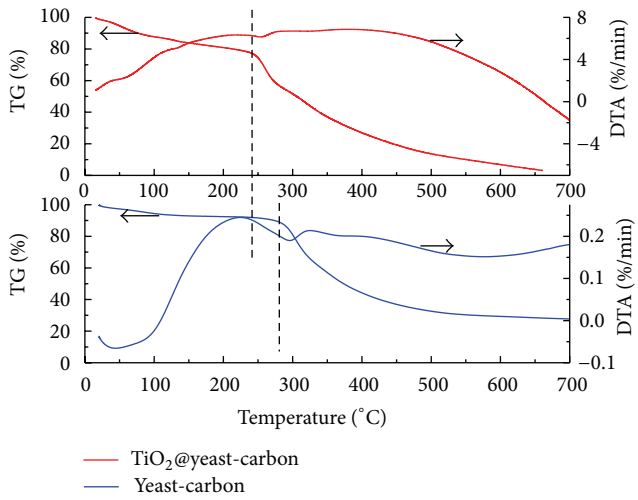

Figure 3: TGA-DTA curves of the yeast and the TiO_2@yeast-carbon.

TiO_2 (JCPDS. No: 21-1276) [25]. The relative intensity of diffraction peaks of TiO_2@yeast carbon is approximately identical with the original components of the TiO_2 as guest particles ($P_{25}TiO_2$: 78% anatase-type TiO_2 and 22% rutile-type TiO_2). The broad peaks at $2\theta = 20^\circ$ in the Figures 2(c) and 2(d) are mainly caused by the amorphous structure of yeast-carbon.

In Figure 3, the distinct decrease in weight of the bare yeast is shown during a wide temperature range of 280–600°C. The rapid weight loss of approximately 50.0% at the temperature range of 280–370°C may be associated with the split of the polysaccharide chains in the yeast [26, 27], which is accompanied by a broad exothermal peak at about 370°C in the DTA curve. The ultimate weight loss from 400 to 600°C can be resulted from the cross-linking of oligosaccharides [28] in the yeast, which is accompanied by the endothermic peak at 500°C in the DTA curve. The total weight loss reaches to about 30.0% and the last weight of the residual ashes is approximately 70.0% of the original yeast biomass. In comparison with the naked yeast, the carbonization reaction of the TiO_2@yeast precursor was started at temperatures about 250°C. The broad exothermal peak at around 200–300°C may be related to the carbonized decomposition of organic substrate in the yeast along with the rapid weight loss of 50.0%. It is worth noting that the broader exothermal peak appeared at around 300–450°C. This may be caused by the release of constitution water and further crystallization of TiO_2 [29]. The wider exothermal peak at 450–600°C can be ascribed to the crystal shift from anatase to rutile phase.

After pyrolysis entirely, the raspberry-like TiO_2@yeast-carbon microspheres can be attained, which has been proved by SEM analysis. The connection between the guest particles TiO_2 and the host particles of the yeast-carbon can be elaborated further by FT-IR analysis. FT-IR spectra of the yeast, yeast-carbon, TiO_2@yeast precursor, TiO_2 and TiO_2@yeast-carbon composites are presented in Figure 4, respectively. For the yeast-carbon, the band around 1570 cm^{-1} can be ascribed to –C=C– stretching bond originated from the inherent structure of yeast, and the bands at 1704 and 1210 cm^{-1} correspond to C=O, C–O stretching of carboxyl groups, respectively [30]. As for TiO_2@yeast-carbon composites, the broad and intense peak at 3500–3200 cm^{-1} can be assigned to the stretching of –OH group due to the bound water in the TiO_2@yeast-carbon composites [31, 32]. The stretching bond corresponding to skeletal Ti–O–Ti is clearly represented in the region of 509 cm^{-1}. The band at 1171 cm^{-1} suggests the presence of C–O bond [33]. The band at around 620 cm^{-1} can be attributed to the Ti–O–C vibration, which indicates that TiO_2 nanoparticles were chemically bonded with yeast-carbon in hybrid particles [34]. Moreover, the band at 3350 cm^{-1} is more prominent in TiO_2@yeast-carbon composites than that of TiO_2, indicating that there were more hydroxyl groups in the TiO_2@yeast-carbon hybrid particles. Generally, more hydroxyl groups lead to generation of more $^{\bullet}OH$ radicals in photocatalysis, which can enhance the photocatalytic activity of TiO_2 [35].

Based on the characterization discussed above, the following mechanism that appeared in Scheme 1 is proposed to account for the formation procedure of the raspberry-like TiO_2@yeast-carbon hybrid microspheres. In Scheme 1, the opposite zeta potentials of yeast cells with a positive charge (H^+) and the nanoparticles TiO_2 with a negative charge (OH^-) were adjusted previously by tuning the pH of their own aqueous suspensions. Then the TiO_2@yeast hybrid precursor with raspberry-like morphology was obtained once the aforementioned aqueous suspensions were mixed [36]. In the obtained raspberry-like TiO_2@yeast precursor, the yeast acted as the host cores and TiO_2 as the guest particles. Afterwards, the carbonization of yeast core in the precursors of raspberry-like TiO_2@yeast can be fulfilled by a gradual temperature-rise procedure, which can obtain the hybrid TiO_2@yeast-carbon composites. TGA-DTA results showed that the final weight loss is approximately 50.0% in the process

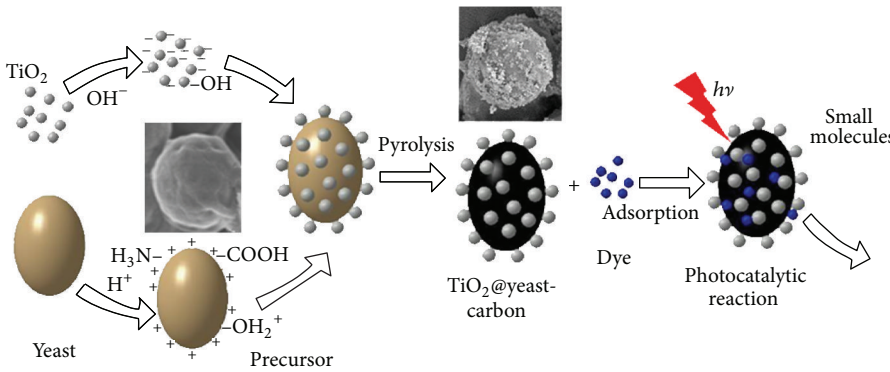

Scheme 1: Schematic illustration for the formation of the raspberry-like TiO_2@yeast-carbon and their synergistic effect in the removal of dyes aqueous solutions.

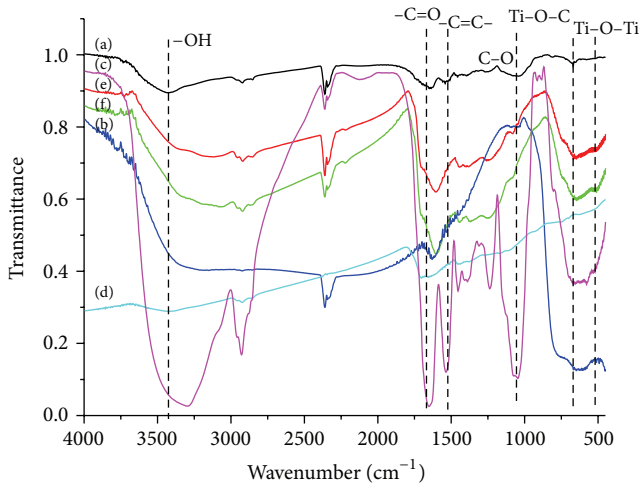

Figure 4: FT-IR spectrum of (a) the original yeast, (b) the TiO_2 nanoparticle, (c) the TiO_2@yeast precursor, (d) the yeast-carbon, (e) the 80% TiO_2@yeast-carbon, and (f) the 40% TiO_2@yeast-carbon.

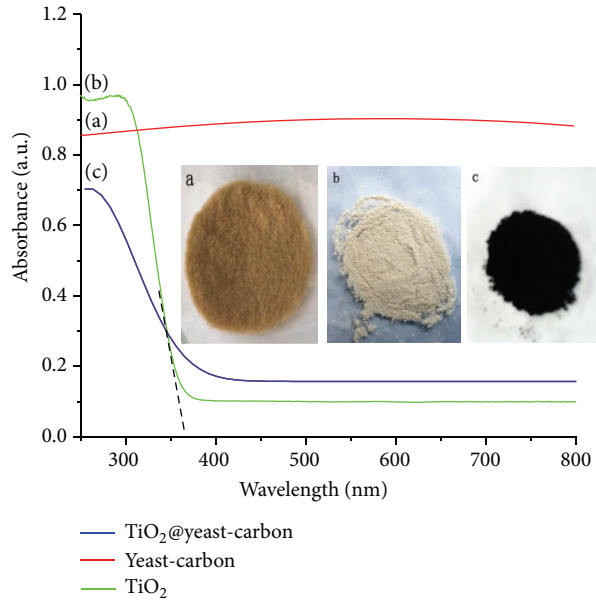

Figure 5: UV-VIS diffuses reflectance spectra of the yeast-carbon, TiO_2 nanoparticles, and the obtained raspberry-like TiO_2@yeast-carbon samples ((a) the yeast-carbon, (b) the TiO_2 nanoparticles, and (c) the hybrid TiO_2@yeast-carbon).

of carbonization. In the obtained raspberry-like TiO_2@yeast-carbon, TiO_2 nanoparticles were chemically bonded with yeast-carbon through FT-IR analysis.

Figure 5 shows the UV-VIS diffuse reflectance spectra of the yeast-carbon, TiO_2 nanoparticles, and the TiO_2@yeast-carbon hybrid particles. In Figure 5(a), the yeast-carbon showed a strong absorption in the range from the UV to the visible light, which was similar to the commercial activated carbon [37]. In Figure 5(b), the band gap energy (E_g) of nanoparticles TiO_2 is estimated about 3.2 ev [38], corresponding to a threshold wavelength of 376 nm. In comparison with the nanoparticles TiO_2, in Figure 5(c), TiO_2@yeast-carbon composites remain optical response in a wide range of 250–400 nm. Besides, in the insert images of Figure 5, the color of the TiO_2@yeast-carbon sample was ash black in comparison with the pure white TiO_2@yeast precursor, which was consistent with its adsorption spectrum.

3.2. Combined Adsorption and Photocatalytic Degradation of Methylene Blue and Congo Red. The raspberry-like TiO_2@yeast-carbon microspheres containing an incompletely covered surface of yeast-carbon may possess unique properties for getting rid of water pollutants. The rich pore structure of yeast-carbon might promote adsorption of organic dyes, while the outer TiO_2 nanoparticles can be in charge of the photocatalytic degradation of the dyes [39]. That is to say that immobilizing TiO_2 nanoparticles on adsorbent-like yeast-carbon can result in a synergistic effect on the efficient degradation of dye in the photocatalytic process. Specially, yeast-carbon core has the capability to extend the separation lifetime of photogenerated e^-/h^+ from outer TiO_2 nanoparticles [40] and thus increasing the quantum efficiency of TiO_2. In turn, TiO_2 nanoparticles can destroy dyes by photocatalytic oxidation, thus regenerating the yeast-carbon in situ. In order to test the activity of the composite TiO_2@yeast-carbon catalysts, the photocatalytic experiments

Table 1: Comparison of the adsorption constant for MB and CR.

Dyes	C_0 (mg/L)	q_e (mg/g)	Langmuir isotherm $C_e/q_e = (1/Q_0b) + (1/Q_0)C_e$			Freundlich isotherm $\ln q_e = \ln K_F + (1/n)\ln C_e$		
			Q_0 (mg/g)	b (1/mg)	R^2	K_F [(mg/g)((1/mg)$^{1/n}$)]	$1/n$	R^2
MB	1.00	0.23	1.53	1.25	0.99	0.78	0.94	0.83
	2.00	0.56						
	3.00	0.87						
	4.00	1.17						
	5.00	1.18						
CR	3.00	0.12	1.15	0.33	0.98	0.39	0.13	0.82
	5.00	0.34						
	7.00	0.59						
	9.00	0.74						
	11.00	0.75						

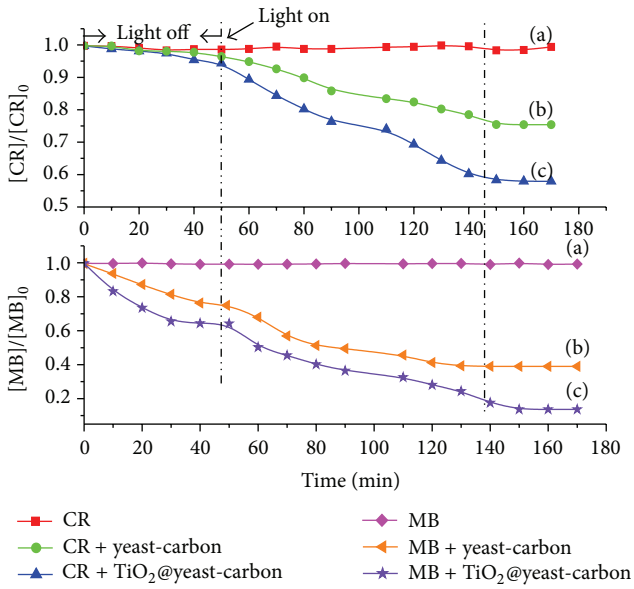

Figure 6: Photocatalytic activities of yeast-carbon and TiO_2@yeast-carbon under UV irradiation.

were carried out for the degradation of MB and CR aqueous solution widely used as model compound for photocatalytic nanomaterial standardization.

From the results shown in Figure 6, the MB and CR aqueous solution is barely photolyzed by UV light irradiation in Figure 6(a). In Figure 6(b) the adsorption-desorption equilibrium was set up within 50.0 min dark environment. The adsorption capacity of the TiO_2@yeast-carbon microspheres for MB was higher than that for CR, which can be assigned to the negatively charged surface of the catalyst. Hereafter, the experiments of the removal of dyes in aqueous solution were preceded for about 120.0 min under UV light irradiation. During 50.0~140.0 minutes, only the adsorption procedures of MB and CR dyes onto the yeast-carbon continuously occurred in the yeast-carbon suspension in Figure 6(b). In the presence of the TiO_2@yeast-carbon catalysts, the adsorption and photocatalysis occurred simultaneously in Figure 6(c). Thus, the degradation rate of the dye in the TiO_2@yeast-carbon catalyst suspension was significantly higher than that in the yeast-carbon suspension. After 140.0 minutes, the adsorption of dyes onto the yeast-carbon tended to reach the adsorption equilibrium. However, the photocatalytic reactions under UV irradiation still proceeded constantly by TiO_2@yeast-carbon catalysts. Finally, approximately 87.0% degradation rate of MB was achieved, whereas only around 30.0% CR was removed from the suspension. The distinct disparity of degradation rate between MB and CR dye aqueous solution can be attributed to their own adsorption performance onto the TiO_2@yeast-carbon catalyst.

The adsorption constant for MB and CRwas listed in Table 1. From the results in Table 1, the maximum adsorption amount of the hybrid TiO_2@yeast-carbon catalysts for cationic MB was significantly higher than that for anionic CR. In addition, the Langmuir model for MB and CR yields a somewhat better fit than the Freundlich model. The value of $1/n$ is equal to 0.94 (MB) and (0.13), respectively, which indicates that the adsorption may belong to the favorable adsorption [41]. This prior adsorption of MB than CR dyes on the surface of the TiO_2@yeast-carbon microspheres may be assigned to the negatively charged properties of composite catalyst. The discriminatory adsorption for the MB and CR dyes by the TiO_2@yeast-carbon composite catalyst inevitably leads to the disparity of above-mentioned photocatalytic degradation rate. Therefore, the adsorption behavior on the surface of the TiO_2@yeast-carbon microspheres has a direct impact on the photocatalytic degradation of the MB and CR dyes.

4. Conclusions

In summary, we prepared hybrid raspberry-like TiO_2@yeast-carbon utilizing pyrolysis method. The as-synthesized hybrid TiO_2@yeast-carbon had ordered elliptic shapes of uniform size (length = 3.7 ± 0.3 μm; width = 2.5 ± 0.5 μm). The potential applications of these novel composites for the removal of contaminants were ascertained for the removal of MB and CR. The results showed that the hybrid composites

exhibited excellent photocatalytic activity for the MB due to its enhanced adsorption ability. The novel TiO_2@yeast-carbon hybrid microspheres have potential applications not only in polluted water treatment but also in other areas such as sensors devices and dye sensitized solar cells.

Acknowledgments

This work was financially supported by China Postdoctoral Science Special Foundation, Scientific Research Foundation for the Returned Overseas Chinese Scholars, the National Natural Science Foundation of China (no. 21176031), Shaanxi Provincial Natural Science Foundation of China (no. 2011JM2011), and Fundamental Research Funds for the Central Universities (no. 2013G2291015).

References

[1] C. L. Wang, J. T. Yan, X. J. Cui, and H. Y. Wang, "Synthesis of raspberry-like monodisperse magnetic hollow hybrid nanospheres by coating polystyrene template with Fe_3O_4@SiO_2 particles," *Journal of Colloid and Interface Science*, vol. 354, no. 1, pp. 94–99, 2011.

[2] M. D'Acunzi, L. Mammen, M. Singh et al., "Superhydrophobic surfaces by hybrid raspberry-like particles," *Faraday Discussions*, vol. 146, pp. 35–48, 2010.

[3] M. Agrawal, A. Pich, N. E. Zafeiropoulos et al., "Polystyrene-ZnO composite particles with controlled morphology," *Chemistry of Materials*, vol. 19, no. 7, pp. 1845–1852, 2007.

[4] X. W. Zhang, M. H. Zhou, and L. C. Lei, "Enhancing the concentration of TiO_2 photocatalyst on the external surface of activated carbon by MOCVD," *Materials Research Bulletin*, vol. 40, no. 11, pp. 1899–1904, 2005.

[5] A. H. El-Sheikh, A. P. Newman, H. Al-Daffaee, S. Phull, N. Cresswell, and S. York, "Deposition of anatase on the surface of activated carbon," *Surface and Coatings Technology*, vol. 187, no. 2-3, pp. 284–292, 2004.

[6] Y. J. Li, X. D. Li, J. W. Li, and J. Yin, "Photocatalytic degradation of methyl orange by TiO_2-coated activated carbon and kinetic study," *Water Research*, vol. 40, no. 6, pp. 1119–1126, 2006.

[7] J. Pouilleau, D. Devilliers, F. Garrido, S. Durand-Vidal, and E. Mahé, "Structure and composition of passive titanium oxide films," *Materials Science and Engineering B*, vol. 47, no. 3, pp. 235–243, 1997.

[8] S. Karuppuchamy, K. Nonomura, T. Yoshida, T. Sugiura, and H. Minoura, "Cathodic electrodeposition of oxide semiconductor thin films and their application to dye-sensitized solar cells," *Solid State Ionics*, vol. 151, no. 1–4, pp. 19–27, 2002.

[9] F.-D. Duminica, F. Maury, and F. Senocq, "Atmospheric pressure MOCVD of TiO_2 thin films using various reactive gas mixtures," *Surface and Coatings Technology*, vol. 188-189, no. 1–3, pp. 255–259, 2004.

[10] C.-S. Kuo, Y.-H. Tseng, C.-H. Huang, and Y.-Y. Li, "Carbon-containing nano-titania prepared by chemical vapor deposition and its visible-light-responsive photocatalytic activity," *Journal of Molecular Catalysis A*, vol. 270, no. 1-2, pp. 93–100, 2007.

[11] B.-Y. Jia, L.-Y. Duan, C.-L. Ma, and C.-M. Wang, "Characterization of TiO_2 loaded on activated carbon fibers and its photocatalytic reactivity," *Chinese Journal of Chemistry*, vol. 25, no. 4, pp. 553–557, 2007.

[12] G. J. Hu, X. F. Meng, X. Y. Feng, Y. F. Ding, S. M. Zhang, and M. S. Yang, "Anatase TiO_2 nanoparticles/carbon nanotubes nanofibers: preparation, characterization and photocatalytic properties," *Journal of Materials Science*, vol. 42, no. 17, pp. 7162–7170, 2007.

[13] J.-H. Liu, R. Yang, and S.-M. Li, "Preparation and application of efficient TiO_2/ACFs photocatalyst," *Journal of Environmental Sciences*, vol. 18, no. 5, pp. 979–982, 2006.

[14] N. Areerachakul, S. Vigneswaran, H. H. Ngo, and J. Kandasamy, "Granular activated carbon (GAC) adsorption-photocatalysis hybrid system in the removal of herbicide from water," *Separation and Purification Technology*, vol. 55, no. 2, pp. 206–211, 2007.

[15] M.-L. Chen, C.-S. Lim, and W.-C. Oh, "Preparation with different mixing ratios of anatase to activated carbon and their photocatalytic performance," *Journal of Ceramic Processing Research*, vol. 8, no. 2, pp. 119–124, 2007.

[16] A. K. Subramani, K. Byrappa, S. Ananda, K. M. Lokanatha Rai, C. Ranganathaiah, and M. Yoshimura, "Photocatalytic degradation of indigo carmine dye using TiO_2 impregnated activated carbon," *Bulletin of Materials Science*, vol. 30, no. 1, pp. 37–41, 2007.

[17] J. M. Dona, C. Garriga, J. Arana et al., "The effect of dosage on the photo-catalytic degradation of organic pollutants," *Research on Chemical Intermediates*, vol. 33, pp. 351–358, 2007.

[18] G. Li Puma, A. Bono, and J. G. Collin, "Preparation of titanium dioxide photocatalyst loaded onto activated carbon support using chemical vapor deposition: a review paper," *Journal of Hazardous Materials*, vol. 157, no. 2-3, pp. 209–219, 2008.

[19] R. Nacco and E. Aquarone, "Preparation of active carbon from yeast," *Carbon*, vol. 16, no. 1, pp. 31–34, 1978.

[20] Z. G. Guan, L. Liu, L. L. He, and S. Yang, "Amphiphilic hollow carbonaceous microspheres for the sorption of phenol from water," *Journal of Hazardous Materials*, vol. 196, pp. 270–277, 2011.

[21] M. Chen, S. X. Zhou, B. You, and L. M. Wu, "A novel preparation method of raspberry-like PMMA/SiO_2 hybrid microspheres," *Macromolecules*, vol. 38, no. 15, pp. 6411–6417, 2005.

[22] W.-C. Oh, J.-G. Kim, H. Kim et al., "Synthesis of spherical carbons containing titania and their physicochemical and photochemical properties," *Journal of the Korean Ceramic Society*, vol. 48, no. 1, pp. 6–13, 2011.

[23] W. Z. Shen, Y. He, S. C. Zhang, J. F. Li, and W. B. Fan, "Yeast-based micro-porous carbon materials for carbon dioxide capture," *ChemSusChem*, vol. 5, pp. 1274–1279, 2012.

[24] A. Pottier, S. Cassaignon, C. Chanéac, F. Villain, E. Tronc, and J.-P. Jolivet, "Size tailoring of TiO_2 anatase nanoparticles in aqueous medium and synthesis of nanocomposites. Characterization by Raman spectroscopy," *Journal of Materials Chemistry*, vol. 13, no. 4, pp. 877–882, 2003.

[25] H. Zhang and J. F. Banfield, "Understanding polymorphic phase transformation behavior during growth of nanocrystalline aggregates: insights from TiO_2," *Journal of Physical Chemistry B*, vol. 104, no. 15, pp. 3481–3487, 2000.

[26] M. Sevilla and A. B. Fuertes, "Chemical and structural properties of carbonaceous products obtained by hydrothermal carbonization of saccharides," *Chemistry*, vol. 15, no. 16, pp. 4195–4203, 2009.

[27] M. B. Wu, "Advance of research in making actived carbon by chemical activation," *Carbon Techniques*, vol. 4, no. 102, pp. 19–23.

[28] N. Baccile, G. Laurent, F. Babonneau, F. Fayon, M.-M. Titirici, and M. Antonietti, "Structural characterization of hydrothermal carbon spheres by advanced solid-state MAS ^{13}C NMR investigations," *Journal of Physical Chemistry C*, vol. 113, no. 22, pp. 9644–9654, 2009.

[29] X.-Y. Deng, Z.-L. Cui, F.-L. Du, and C. Peng, "Thermal analysis characterization of nanosized TiO_2," *Journal of Inorganic Materials*, vol. 16, no. 6, pp. 1089–1093, 2001.

[30] R. Gnanasambandam and A. Proctor, "Determination of pectin degree of esterification by diffuse reflectance Fourier transform infrared spectroscopy," *Food Chemistry*, vol. 68, no. 3, pp. 327–332, 2000.

[31] S. D. Jacobsen, S. Demouchy, D. J. Frost, T. B. Ballaran, and J. Kung, "A systematic study of OH in hydrous wadsleyite from polarized FTIR spectroscopy and single-crystal X-ray diffraction: oxygen sites for hydrogen storage in Earth's interior," *American Mineralogist*, vol. 90, no. 1, pp. 61–70, 2005.

[32] P. C. Painter, R. W. Snyder, M. Starsinic, M. M. Coleman, D. W. Kuehn, and A. Davis, "Concerning the application of FT-IR to the study of coal: a critical assessment and band assignments and the application of spectral analysis programs," *Applied Spectroscopy*, vol. 35, no. 5, pp. 475–485, 1981.

[33] W. Jiang, J. Joens, D. D. Dionysiou, and K. E. O'Shea, "Optimization of photocatalytic performance of TiO_2 coated glass microspheres using response surface methodology and the application for degradation of dimethyl phthalate," *Journal of Photochemistry and Photobiology A*, vol. 262, pp. 7–13, 2013.

[34] Y. F. Zhu, L. I. Zhang, C. Gao, and L. L. Cao, "The synthesis of nanosized TiO_2 powder using a sol-gel method with $TiCl_4$ as a precursor," *Journal of Materials Science*, vol. 35, no. 16, pp. 4049–4054, 2000.

[35] Y.-J. Li, Z.-J. Song, Z.-P. Li, Y.-Z. Ouyang, and W.-B. Yan, "Preparation and photocatalytic properties of activated carbon supported TiO_2 nanoparticles with cu ions doping," *Chemical Journal of Chinese Universities*, vol. 28, no. 9, pp. 1710–1715, 2007.

[36] B. Bai, N. Quici, Z. Y. Li, and G. L. Puma, "Novel one step fabrication of raspberry-like TiO_2@yeast hybrid microspheres via electrostatic-interaction-driven self-assembled heterocoagulation for environmental applications," *Chemical Engineering Journal*, vol. 170, no. 2-3, pp. 451–456, 2011.

[37] Y. Q. Gai, J. B. Li, S.-S. Li, J.-B. Xia, and S.-H. Wei, "Design of narrow-gap TiO_2: a passivated codoping approach for enhanced photoelectrochemical activity," *Physical Review Letters*, vol. 102, no. 3, Article ID 036402, 4 pages, 2009.

[38] M. Takeuchi, K. Sakamoto, G. Martra, S. Coluccia, and M. Anpo, "Mechanism of photoinduced superhydrophilicity on the TiO_2 photocatalyst surface," *Journal of Physical Chemistry B*, vol. 109, no. 32, pp. 15422–15428, 2005.

[39] J. Matos, A. Garcia, T. Cordero, J.-M. Chovelon, and C. Ferronato, "Eco-friendly TiO_2-AC photocatalyst for the selective photooxidation of 4-chlorophenol," *Catalysis Letters*, vol. 130, no. 3-4, pp. 568–574, 2009.

[40] Z. B. Zhang, C. C. Wang, R. Zakaria, and J. Y. Ying, "Role of particle size in nano-crystalline TiO_2-based photo-catalysts," *The Journal of Physical Chemistry B*, vol. 52, pp. 10871–10878, 1998.

[41] R. J. Umpleby II, S. C. Baxter, Y. Z. Chen, R. N. Shah, and K. D. Shimizu, "Characterization of molecularly imprinted polymers with the Langmuir—freundlich isotherm," *Analytical Chemistry*, vol. 73, no. 19, pp. 4584–4591, 2001.